

UNCLASSIFIED

AD NUMBER	
AD011594	
CLASSIFICATION CHANGES	
TO:	unclassified
FROM:	confidential
LIMITATION CHANGES	
TO:	Approved for public release, distribution unlimited
FROM:	Distribution authorized to U.S. Gov't. agencies and their contractors; Administrative/Operational Use; FEB 1953. Other requests shall be referred to Naval Ordnance Systems Command, Washington, DC.
AUTHORITY	
28 Feb 1965 per Group-4, DoDD 5200.10; Naval Ordnance Lab ltr dtd 26 Aug 1974	

THIS PAGE IS UNCLASSIFIED

Reproduced by

— Armed Services Technical Information Agency
DOCUMENT SERVICE CENTER

KNOTT BUILDING, DAYTON, 2, OHIO

AD -

1 1 5 9 4

CONFIDENTIAL

CONFIDENTIAL

NAVORD REPORT 2768

12808

AD No. 17594
ASTIA FILE COPY
RAPID EXPANSION OF METAL CYLINDERS UNDER EXPLOSIVE LOADING I
STUDIES OF INITIAL EXPANSIONS WITH THE ROTATING MIRROR CAMERA

4 February 1953



U. S. NAVAL ORDNANCE LABORATORY
WHITE OAK, MARYLAND

CONFIDENTIAL

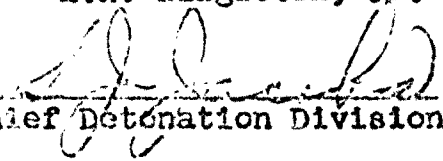
SECURITY INFORMATION

CONFIDENTIAL
NAVORD Report 2768

RAPID EXPANSION OF METAL CYLINDERS UNDER EXPLOSIVE LOADING I
STUDIES OF INITIAL EXPANSIONS WITH THE ROTATING MIRROR CAMERA

Prepared by:

A.D. Solem
B.H. Singleton, Jr.

Approved by: 

Chief Detonation Division

ABSTRACT: The expansion rates of steel and aluminum cylinders (2.0 inch inside diameter with wall thicknesses between 0.0 to 0.5 inch) when accelerated by detonation of Composition B explosive filling have been studied before a rotating mirror-slit camera. These data are desired for an accurate determination of initial fragment velocities and accelerations. A comparison is made of the observed values, the Gurney velocities, and the fragment velocities measured on the NOL fragment velocity range. By proper choice of the Gurney constant, the velocities calculated by the Gurney formula may be brought into good agreement with the observed values in the region above 0.05 inches wall for steel, and 0.1 inch wall for aluminum. For thinner cases the observed velocities diverge considerably from the Gurney predicted values. A discussion is given concerning the effectiveness of the rotating mirror camera in fragmentation work and the errors and assumptions which enter into interpretation of the data obtained.

EXPLOSIVES RESEARCH DEPARTMENT
U.S. NAVAL ORDNANCE LABORATORY
WHITE OAK, MARYLAND

1

CONFIDENTIAL
SECURITY INFORMATION

CONFIDENTIAL

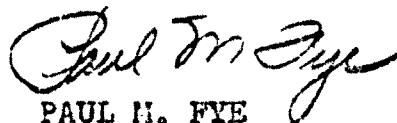
NAVORD Report 2768

4 February 1953

The work presented in this report has been undertaken for the purpose of investigating initial velocities of fragments coming from expanding cylinders over a range of wall thicknesses down to zero wall. The problem has been considered by earlier workers, but not in detail. References (a), (e), (f), and (g) at the end of this report give the earlier work. This investigation has been performed under Task NOL-Re2c-35-1-53. The data presented and the conclusions drawn are of a preliminary nature.

The authors wish to acknowledge the assistance of T.P. Liddiard who furnished many valuable experimental techniques. The authors also are indebted to D. Danielson and H. Curtis who did much of the experimental work, and T.W. Froyd who assisted in analysis of the data.

EDWARD L. WOODYARD
Captain, USN
Commander



PAUL H. FYE
By direction

CONFIDENTIAL
NAVORD Report 2768

CONTENTS

	Page
Introduction	1
Experimental Procedure and Computations	2
Test Arrangement	2
Computation of Velocities	3
Discussion of Experimental Results	4
Extent of Tests	4
Helium Atmosphere	6
Nature of Results	6
Summary	8
Appendix	19

ILLUSTRATIONS

Table I. Aluminum and Steel Cylinder Velocities in Air	9
Table II. Aluminum Cylinder Velocities in Helium	10
Table III. Twelve Inch Aluminum Cylinder Velocities	10
Table IV. Average Velocities for Aluminum and Steel Cylinders in Helium and Air	11
Table V. Comparison of Velocities Measured by Rotating Mirror Camera and Fragment Velocity Range	11
Figure 1. Shadow Techniques for Observing Initial Cylinder Velocities	12
Figure 2. Comparison of Records in Helium and Air Atmospheres for Expansion of Uncased Explosive	13
Figure 3. Comparison of Records in Helium and Air Atmosphere for Expansion of 0.005 in. Aluminum Cylinder	14
Figure 4. Translation from Moving Coordinate System to Fixed Coordinate System in Calculating Cylinder Velocity	15
Figure 5. Comparison of Observed Velocities with Gurney Velocities	16
Figure 6. Observed Velocities as a Function of Equivalent Mass of Steel	16
Figure 7. Average g vs t Plot for Expansion of Steel Cylinders of Various Wall Thicknesses	17
Figure 8. Average y vs t Plot for Expansion of Aluminum Cylinders of Various Wall Thicknesses	18
Figure 9. Distortion of Observed Cylinder Radius Produced by Change of Refractive Index	22
Figure 10. The Effect of Finite Initial Shock Radius on the Distortion of the Observed Cylinder Radius	23

CONFIDENTIAL
NAVORD Report 2768

RAPID EXPANSION OF METAL CYLINDERS UNDER EXPLOSIVE LOADING I
STUDIES OF INITIAL EXPANSIONS WITH THE ROTATING MIRROR CAMERA

INTRODUCTION

1. Knowledge of fragment accelerations and velocities from cases under explosive loading is required in any fragmentation or explosive-metal interaction study. The earlier work of Gurney, Reference (a), has been of considerable value in attempting to predict initial fragment velocities from cylindrical cases. Included in his formula was a multiplying constant which was different for each explosive and was obtained by curve-fitting to observed data. It was also stated by Gurney that agreement with experimental velocities would not necessarily extrapolate to zero wall thickness where little data were available. The departure of the predicted Gurney velocities from observed velocities was considered of sufficient importance to be further investigated, because such studies would lead to a more detailed consideration of the hydrodynamic process involved. It could also lead to a better understanding of the fragmentation of cased charges other than those having cylindrical symmetry.
2. Conventional methods of measuring fragment velocities, References (b), (c) and (d), are not satisfactory for thin walled cases due to difficulty in observing small fragments in motion. Expanding cylinders have been studied with primacord-shutter camera and exploding flash lamps, Reference (e) through (g). The resolution obtained in this work is, however, rather poor. It was believed that a rotating mirror--slit camera, Reference (h), could be used with greater resolution since a similar arrangement has previously been used successfully with a rotating drum--slit camera to study shock from charges detonated in air, Reference (i). A secondary purpose of the test was to investigate the rotating mirror--slit camera as a fragmentation tool in which the nature of fragment accelerations could be resolved.
3. In the present series of tests, fragment velocities after acceleration have been obtained for 2 inch inside diameter steel and aluminum cylinders of different wall thicknesses when expanded by detonation of Composition B explosive. These velocities are compared to the predicted values and the point of departure of the Gurney formula noted. The results obtained are also compared, after application of retardation theory, Reference (j), to the velocities obtained for similar cylinders on the NOL fragment

CONFIDENTIAL
NAVORD Report 2768

velocity range. Agreement is good for steel fragments where the retardation effect is fairly well known. The agreement for aluminum fragments also appears to be satisfactory for the amount of information available on this type of fragment. On the basis of other unpublished work at NOL concerning shock reflections in metals, it was expected that velocity jumps would be observed in this method of observing fragment velocities. However, up to the present time, such velocity changes have not been clearly noted. As a matter of definition, by initial case velocity is meant the velocity of initial expansion. Terminal case velocity is defined as that velocity at which the case vents. The terminal case velocity is therefore the initial fragment velocity.

EXPERIMENTAL PROCEDURE & COMPUTATIONS

4. Test Arrangement. Figure 1 shows the general experimental arrangement used in these tests. The cased charge was mounted on a stand inside the bombproof such that the cross-section of the cylinder to be observed was in the slit line projected out from the camera. The axis of the cylinder was oriented perpendicular to the slit line in a horizontal plane. The cylinder was back-lighted by an exploding wire light source, Reference (k), also located along the projected slit line. A mirror on the stand permitted orientation of the cylinder so that fragments would not fly into the bombproof window which protected the camera. The window was further protected by a thin sheet of lucite which stopped occasional ricochets and fogging by explosive gases.

5. A standard rotating mirror--slit camera, Reference (h), outside the bombproof was used to record the expansion. It contains a slit which is perpendicular to the image travel on the film drum. The light and explosive charge were synchronously triggered so that the light flashed just as the detonation swept past the point of the cylinder under observation. A silhouette of the case motion as a $y-t$ plot at the slit line was obtained on the film. Figures 2 and 3 show typical enlargements of the records. The camera was focused on the top surface of the case to give a sharp silhouette. The slit width was that ordinarily used in detonation studies with the camera. The records were considered satisfactory without further adjustment. A still picture of the charge was taken at one end of the film. This picture was used to compute the object-image ratio of the streak record.

CONFIDENTIAL
NAVORD Report 2768

6. Computation of Velocities. The method by which the camera data were reduced to the apparent case velocities along the slit was conventional. The negatives were enlarged to give a one and a half to double magnification of the original cylinder size and a plot was made of y vs t . Distances along the y direction of the print scaled directly to distances on the plot with multiplication by the magnification factor. The time axis of the camera is a calibrated function of rotor speed and drum radius. Thus distances along the t direction of the print scaled directly to time on the plot by use of an accurately known enlarging factor. In this camera, the reflecting surface of the mirror does not rotate on the axis of the film drum, therefore, the magnification is a function of distance along the film. The records, however, were of such a short length that no correction had to be made. (Units changed less than 0.2 per cent over the record). From the y vs t plot the case velocity was calculated at any point as $\Delta y / \Delta t$. Principle interest at this time was in the terminal velocity of the case expansion. This is the velocity after acceleration had taken place, and was computed from the straight line region of the records just before the explosive gases vented through the cracks in the cylinder. In most instances this venting point was easy to locate. The records also showed the mode of acceleration of the case. It is planned to analyze this phase of the case studies in the future.

7. The photographic records gave an apparent velocity along the slit. This, however, was not the true velocity of the expanding cylinder. As the cylinder expanded radially it stretched little, if any, along its length. Thus, with respect to the slit, the point of the cylinder originally under observation moved, after the detonation passed, in the direction of detonation as well as outward. As the expansion increased, the points of the cylinder at the slit came from earlier accelerated regions of the cylinder. The apparent velocity was therefore greater than the true velocity of any one point of the cylinder since the method of recording shortens the time coordinates.

8. The case velocities can be computed if it is assumed that the case expands as an inelastic but plastic medium in the manner given by Taylor, Reference (1). The coordinate system is changed from one at rest with the detonation front to at rest with the cylinder or slit. In Taylor's theory, working with the detonation front at rest and assuming steady state conditions, the initial fragment velocity is given by:

$$V_i = 2D \sin \frac{\alpha}{2}$$

CONFIDENTIAL
NAVORD Report 2768

Here D is the detonation velocity and α is the angle the cylinder wall makes with the cylinder axis after detonation (instantaneous picture of expanding cylinder). Consider now the system with coordinates at rest with respect to the slit. In time Δt the detonation point has moved a distance $\Delta x = D \Delta t$ past the slit, taking t equal to zero as the time at which the detonation passes the slit. In this same time, the cylinder has expanded a distance Δy on the slit. From Figure (4) it is seen that

$$\alpha = \arctan \frac{\Delta y}{\Delta x} = \arctan \frac{\Delta y}{D \Delta t}.$$

The apparent velocity, v_a , computed from the photographic negative is

$$v_a = \frac{\Delta y}{\Delta t}.$$

Therefore

$$\alpha = \arctan \frac{v_a}{D},$$

and the true initial fragment velocity is

$$v_i = 2D \sin \left[\frac{\arctan \left(\frac{v_a}{D} \right)}{2} \right].$$

DISCUSSION OF EXPERIMENTAL RESULTS

9. Extent of Tests. The cases were loaded with Composition B explosive, with cast density of 1.68 grams/centimeter³ and a computed detonation velocity of 7850 meters/second. Expansions for the following cylinders have been obtained:

- (a) In air. Length, 5.0 inches; inside diameter, 2.0 inches; slit location, at center of cylinder.

Wall Thicknesses in Inches

<u>Aluminum</u>	<u>Steel</u>
0.062	0.031
0.125	0.062
0.250	0.125
0.375	0.250
0.500	

CONFIDENTIAL
NAVORD Report 2768

- (b) In helium (atmosphere pressure). Length; 5.0 inches; inside diameter, 2.0 inches; slit location, at center of cylinder

Wall Thicknesses in Inches
(Aluminum Cases Only)

0.000 (uncased)
0.002
0.005
0.125
0.250

- (c) In helium and air. Length 12.0 inches; inside diameter, 2.0 inches; slit location 2.5 inches from free end

Wall Thicknesses in Inches
(Aluminum Cases Only)

Uncased in helium
0.125 in air
0.500 in air.

Initiation was by a pentolite-baratol plane wave booster. The aluminum cylinders were machined from 2-S seamless tubing; the steel cylinders were machined from AISI 1045, stress relief seamless tubing in the as-is condition (Rockwell 30-B). Tables I, II, and III give experimental apparent and corrected initial fragment velocities for the individual charges. The initial fragment velocities calculated by the Gurney formula for the cylinders are also given for comparison. The average velocities for each of the different conditions are given in Table IV.

10. It is to be noted that there is considerable spread in the results from identical shots. The photographic records can be analyzed to an accuracy of better than 1 per cent. It is further believed that the experimental technique measures velocities to an accuracy of better than 3 to 4 per cent. Therefore, all of the spread cannot be attributed to measurement errors. Actual differences in the velocities may be caused by small variations in the cases, the explosive, and the interaction of explosive gases with the expanding cases. This is a problem even more acute in ordinary fragment velocity measurements where velocity spreads on the order of 25 per cent are obtained for fragments from one case. The test conditions here have been standardized as

CONFIDENTIAL
NAVORD Report 2768

far as seemed practicable. The velocities obtained are taken as representative values for individual cases. The representative velocity for any set of experimental conditions is taken as the mean of the individual values. A reproducibility study would be needed to show the validity of this assumption.

11. Helium Atmosphere. Air was a satisfactory atmosphere in which to observe the expansion of these cylinders except when the cylinder walls were thin (0.1 inch or so). The shock in front of the expanding cylinder then became so luminous that the cylinder motion could not be followed. Several shots in addition to those given in Table I have been fired, but they had to be discarded because the records could not be used for this reason. The series of shots in helium were fired to test helium as a substitute atmosphere. There is little or no luminosity from helium in the region of initial expansion, even down to the uncased charges. Helium, therefore, can be used as the atmosphere whenever air is unsuitable. A little experience will give the wall thickness at which the change from air to helium must be made. The experiment was not accurate enough to detect the difference between expansions into helium and into air for the thicker cases. For the uncased charges, the expansion into air was so masked by shock light that no comparison was attempted. The series of shots with the long cylinders were fired to see if steady state conditions were obtained when the short cylinders were used. There was no evidence to indicate a lack of steady state for the short cylinders. This was as expected since plane wave boosters were used for initiation.

12. Nature of Results. Figure 5 shows a plot of the initial fragment velocities as a function of case wall thickness. Compared with these are values of velocities for similar cases calculated by the Gurney formula, Reference (a),

$$V = K \left[\frac{C/M}{1 + C/2M} \right]^{1/2},$$

where C and M are the explosive and case weights per unit length respectively, and the constant K has the value 9500 feet/second. Better agreement of the Gurney velocities with the observed velocities is obtained if a value of 8350 to 8500 feet/second is used for K . The fit holds only for the thicker walled cylinders. The Gurney formula does not predict the velocities for cases of wall thickness less than 0.1 inch. Figure 6 gives a comparison of observed initial fragment velocities as a function of equivalent cylinder weight for the

CONFIDENTIAL
NAVORD Report 2768

two types of cylinder. It appears that only the mass of the cylinder wall is important in influencing fragment velocities. The physical properties of the wall enter as higher order effects.

14. While the nature of the wall accelerations has been noted, it has not been considered in detail. Figures 7 and 8 show the mean expansions along the slit line for the different cylinders. The acceleration jumps which have been observed here at NOL in studying detonation interaction with thin aluminum plates at normal incidence were not apparent in the case expansions. It may be that in the present experiment, the jumps are not as pronounced as in the plate experiment, or it may be that the resolution of the system is not sufficient for this observation.

15. For comparison, the initial fragment velocities measured with the rotating mirror camera have been compared to the velocities of fragments from identical cylinders measured in the NOL fragment range. Table V indicates the cylinder sizes considered and shows the velocity comparison. The methods of measuring velocities are not identical in that the former gives the initial fragment velocities and the latter gives the velocities about 9 feet from the cylinder. Some type of retardation adjustment must be used to translate the second group of velocities back to the cylinder for direct comparison. Assuming a standard retardation law, Reference (m), the adjustment is

$$V_{\text{range}} = V_{\text{initial}} e^{-K \rho \frac{A}{m} s},$$

where K is the drag coefficient, A is mean presented area of the fragment, m its mass, ρ the density of air, and s the distance of travel. The exponents $-K \rho \frac{A}{m} s$ and the $K \frac{A}{m}$ values needed for agreement are given in Table V. For the 0.25 inch steel cylinder these are the values for a roughly cubical fragment of mass 1.5 grams with drag coefficient of 0.4. For the aluminum cylinders the exponents and hence the $K \frac{A}{m}$ values are much larger than experience with steel fragments would indicate. For aluminum fragments as for steel fragments it is believed that K should be somewhere between 0.4 and 0.6. This means that the ratio A/m is large for aluminum fragments implying a large presented area and/or a small mass. The range records show that the larger aluminum fragments travel in a manner to maximize presented area. Recovered fragments show extensive thinning of the wall (a low mass). On this evidence the comparisons are considered reasonable.

SUMMARY

16. It has been demonstrated that the Gurney formula does not appear valid when very thin cases are considered. The nature of the departure has been shown for 2.0 inch inside diameter steel and aluminum cylinders loaded with Composition B explosive accelerated by a plane wave detonation directed along the axis. It is assumed in the Gurney development that the contribution to the kinetic energy of the system made by the detonation of each unit mass of explosive is the same in all types of projectiles. The kinetic energy per unit length is then equated to the explosive energy. It is also assumed that the gas velocity is proportional to the distance from the axis of the cylinder. However, the Gurney explosive constant, which is proportional to the square root of the explosive energy, must be calculated from experimental data. It is possible that for thin-walled cases, the kinetic energy distribution of the system is changed so that the explosive factor is no longer constant.

17. These tests have also demonstrated that the rotating mirror-slit camera can be used profitably to study the problems associated with cylinder expansions and initial fragment velocities. The system does have limitations: (a) only one expansion or velocity is obtained per shot and (b) the range of expansion or fragment travel is small. However, it can be adapted to problems which cannot be handled otherwise and it will furnish data of a type not duplicated by other means.

CONFIDENTIAL
NAVORD Report 2768

TABLE I

ALUMINUM AND STEEL CYLINDER VELOCITIES IN AIR
(2 inch ID; Composition B Explosive)

Case Material	Wall Thickness (in)	Apparent Velocity (m/sec)	Initial Velocity (m/sec)	Gurney Velocity (m/sec)
Steel	0.03125 (1/32)	3290	3090	3240
		3390	3180	3240
	0.0625 (1/16)	2570	2470	2770
		2270	2200	2760
		2280	2210	2750
		2600	2500	2760
		2500	2410	2750
	0.125 (1/8)	1960	1920	2200
		2000	1950	2190
		1940	1900	2200
	0.250 (1/4)	1320	1310	1670
		1430	1410	1660
Aluminum	0.0625 (1/16)	4200	3810	3450
		4100	3730	3430
		4090	3720	3440
	0.125 (1/8)	3060	2900	3090
		3030	2880	3110
		3390	3180	3110
	0.250 (1/4)	2270	2200	2460
		2330	2260	2460
		2200	2140	2460
	0.375 (3/8)	1820	1790	2090
		1990	1940	2090
		1900	1860	2090
	0.500 (1/2)	1610	1590	1830
		1560	1540	1830
		1500	1480	1830

CONFIDENTIAL
NAVORD Report 2768

TABLE II

ALUMINUM CYLINDER VELOCITIES IN HELIUM
(2 inch ID; Composition B Explosive)

Wall Thickness (in)	Apparent Velocity (m/sec)	Calculated Initial Velocity (m/sec)	Gurney Velocity (m/sec)
0.0	9580	6720	4090
0.002	9200 8890	6570 6460	4060 4060
0.005	7660 6730	5920 5450	4000 4020
0.125	2990	2840	3070
0.250	2280	2210	2440

TABLE III

TWELVE INCH ALUMINUM CYLINDER VELOCITIES
(2 inch ID; Composition B Explosive)

Wall Thickness (in)	Apparent Velocity (m/sec)	Calculated Initial Velocity (m/sec)	Gurney Velocity (m/sec)
0.0	9880	6820	4090
0.125	3280	3080	3010
0.500	1640 1610	1610 1580	1820 1820

CONFIDENTIAL
NAVORD Report 2768

TABLE IV

**AVERAGE VELOCITIES FOR ALUMINUM AND STEEL
CYLINDERS IN HELIUM AND AIR
(2 inch ID; Composition B Explosive)**

Case Material	Wall Thickness (in)	Medium	Initial Velocity (m/sec)	Gurney Velocity (m/sec)
Uncased Steel	0.0	He	6770	4090
	0.03125	Air	3140	3240
	0.0625	Air	2360	2760
	0.125	Air	1920	2200
Aluminum	0.250	Air	1360	1670
	0.002	He	6520	4060
	0.005	He	5690	4010
	0.0625	Air	3750	3440
	0.125	Air, He	2980	3070
	0.250	Air, He	2200	2460
	0.375	Air	1860	2090
	0.500	Air	1570	1820

TABLE V

**COMPARISON OF VELOCITIES MEASURED BY ROTATING
MIRROR CAMERA AND FRAGMENT VELOCITY RANGE**

Case	Wall Thickness	Initial Velocity (m/sec)	Range Velocity (m/sec)	$-K\rho_m^A s$ for adjustment	$K \frac{A}{m}$
Steel	0.25	1360	1300	0.041	0.119
Aluminum	0.125	2980	1880	0.459	1.326
	0.25	2200	1450	0.417	1.204
	0.375	1860	1340	0.330	0.953
	0.50	1560	1200	0.262	0.758

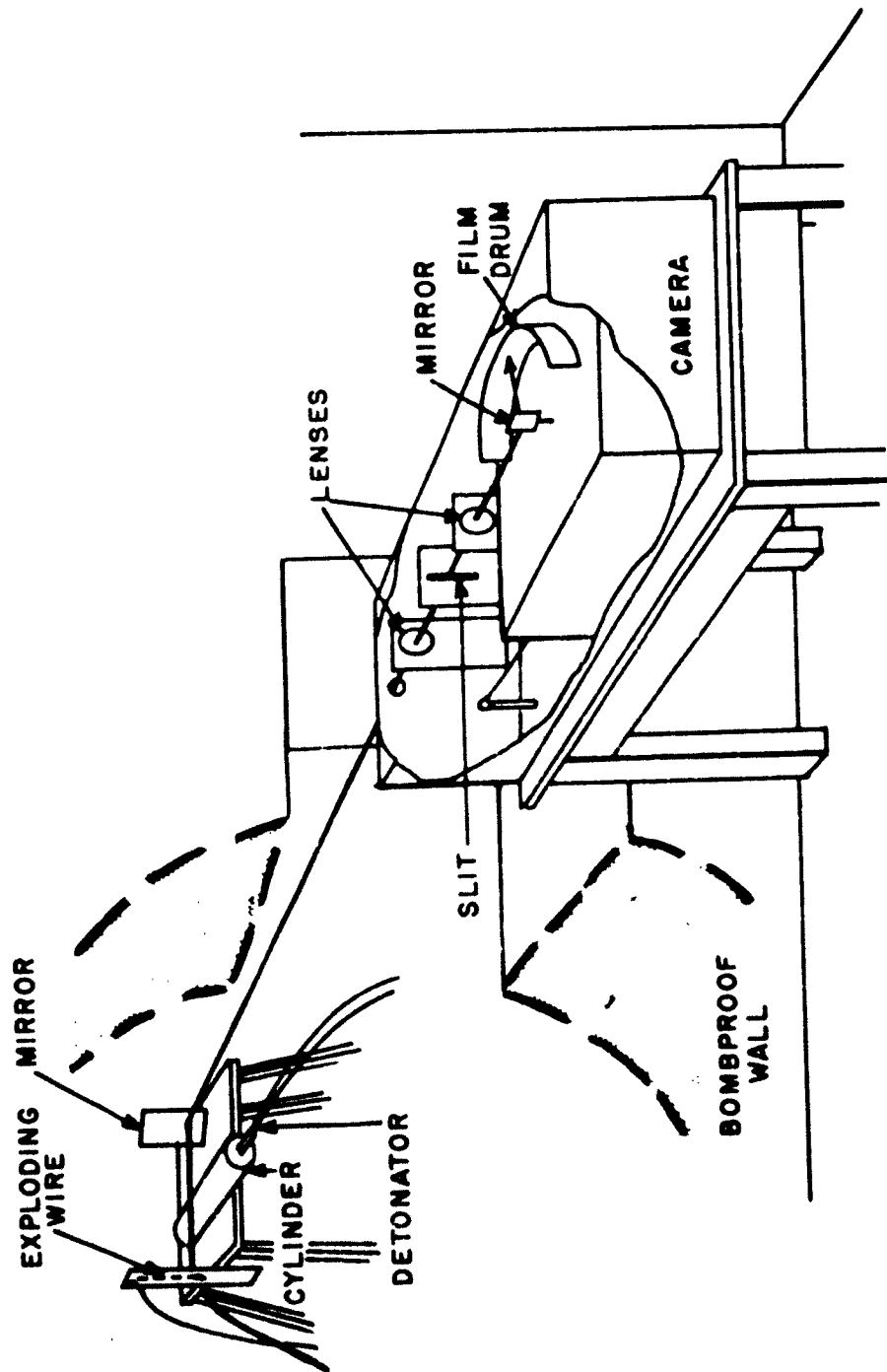


FIG.1 SHADOW TECHNIQUE FOR OBSERVING INITIAL CYLINDER VELOCITIES



(a) AIR ATMOSPHERE



(b) HELIUM ATMOSPHERE

FIG. 2 COMPARISON OF RECORDS IN HELIUM AND AIR ATMOSPHERES
FOR EXPANSION OF UNCASSED EXPLOSIVE



(a) AIR ATMOSPHERE



(b) HELIUM ATMOSPHERE

FIG.3 COMPARISON OF RECORDS IN HELIUM AND AIR ATMOSPHERES
FOR EXPANSION OF 0.005 IN. ALUMINUM CYLINDER

SECURITY
INFORMATION

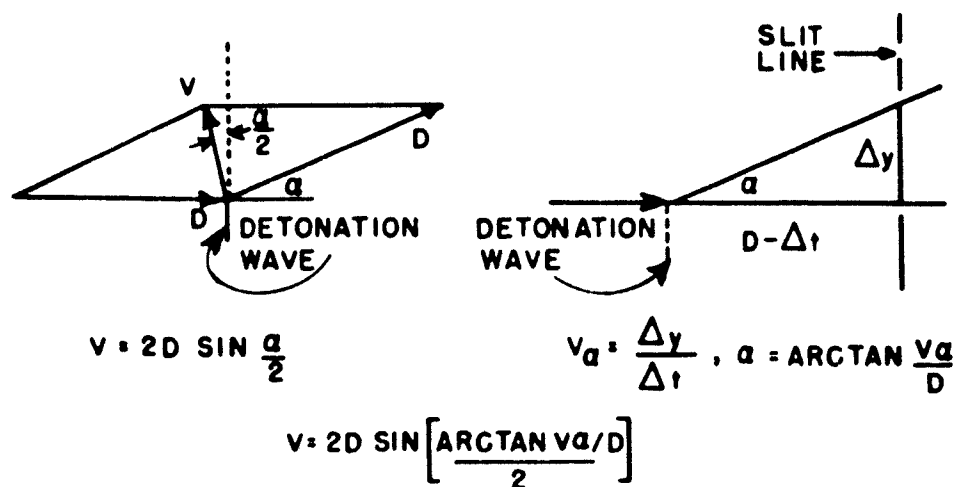


FIG. 4 TRANSLATION FROM MOVING COORDINATE SYSTEM TO
FIXED COORDINATE SYSTEM IN CALCULATING CYLINDER VELOCITY

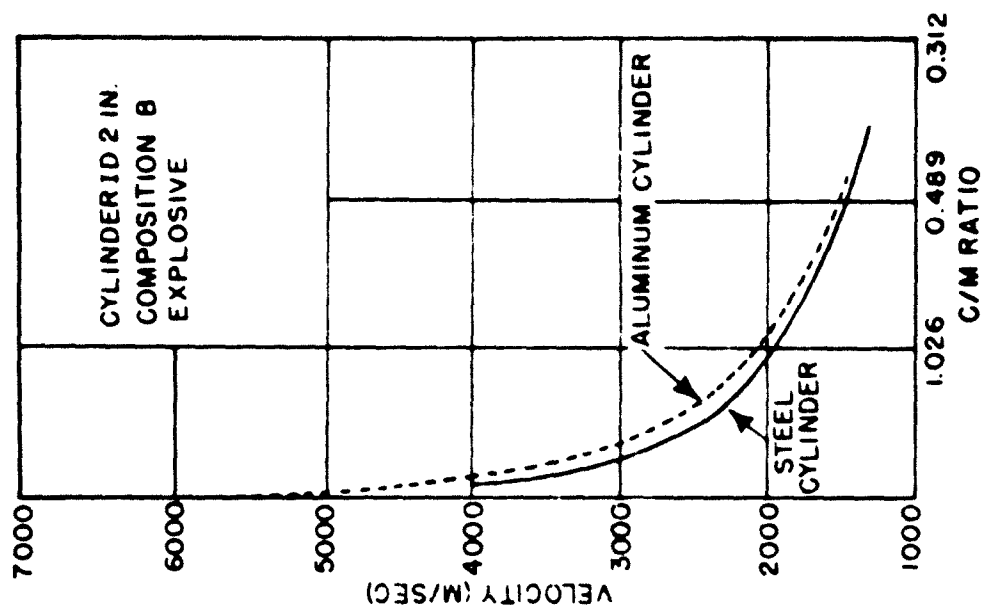


FIG. 6 OBSERVED VELOCITIES AS A FUNCTION OF EQUIVALENT MASS OF STEEL

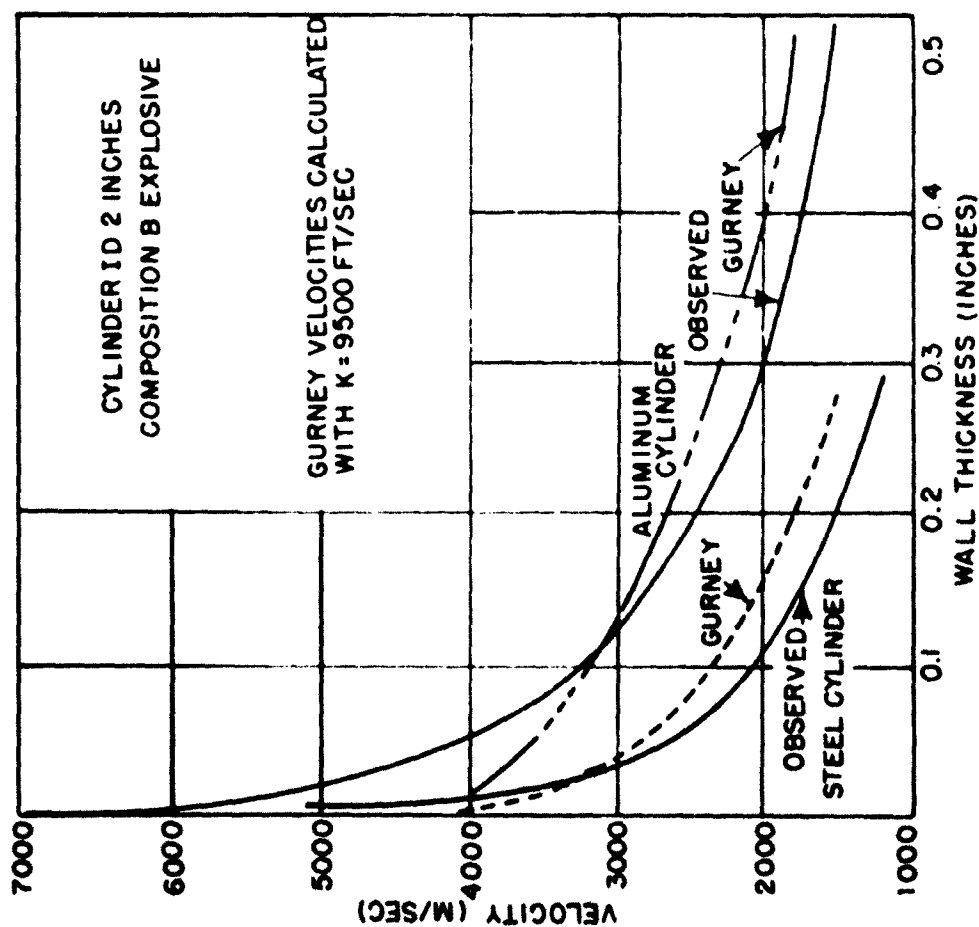


FIG. 5 COMPARISON OF OBSERVED VELOCITIES WITH GURNEY VELOCITIES

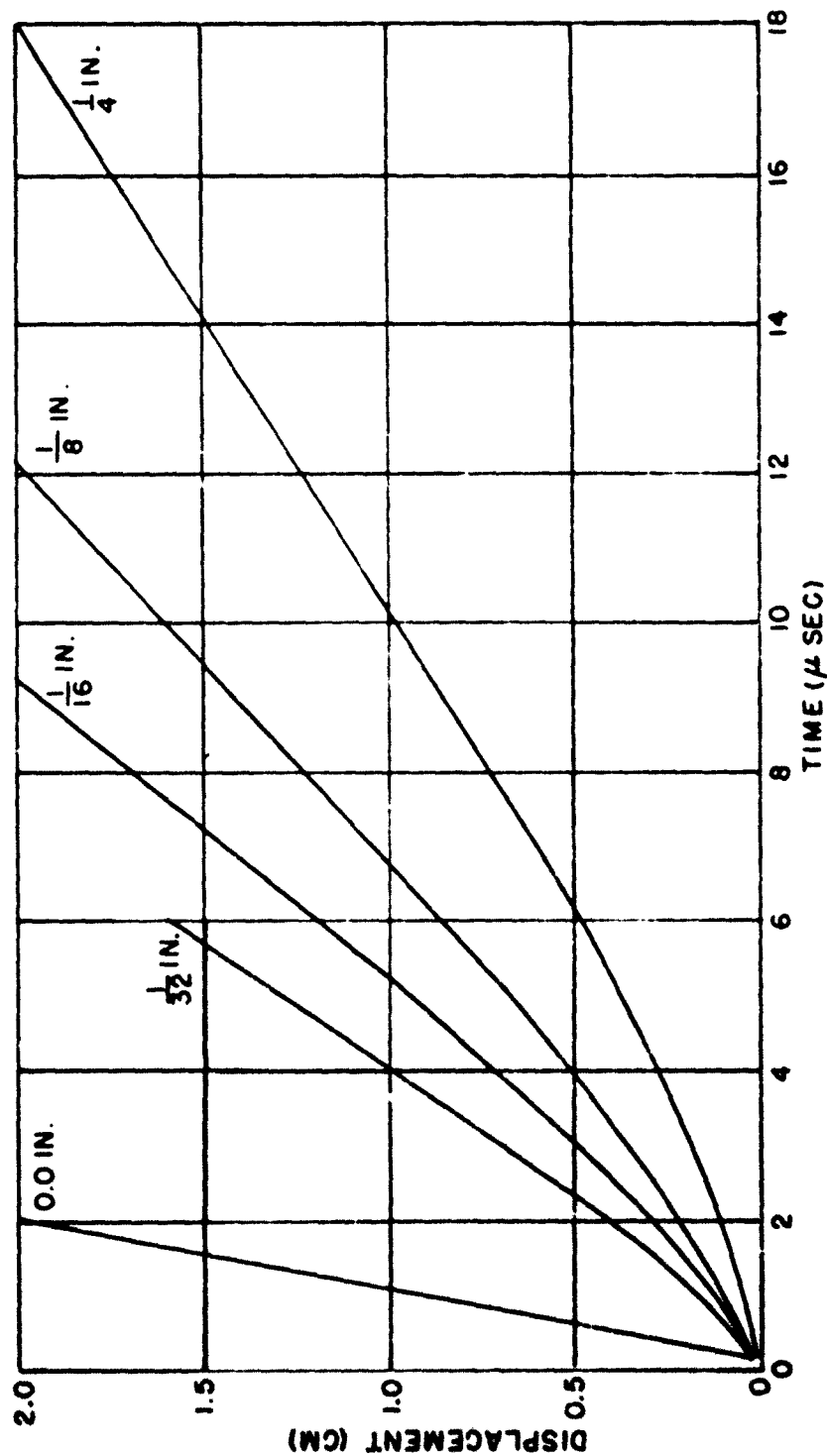


FIG. 7 AVERAGE Y VS T PLOT FOR EXPANSION OF STEEL CYLINDERS OF VARIOUS WALL THICKNESSES

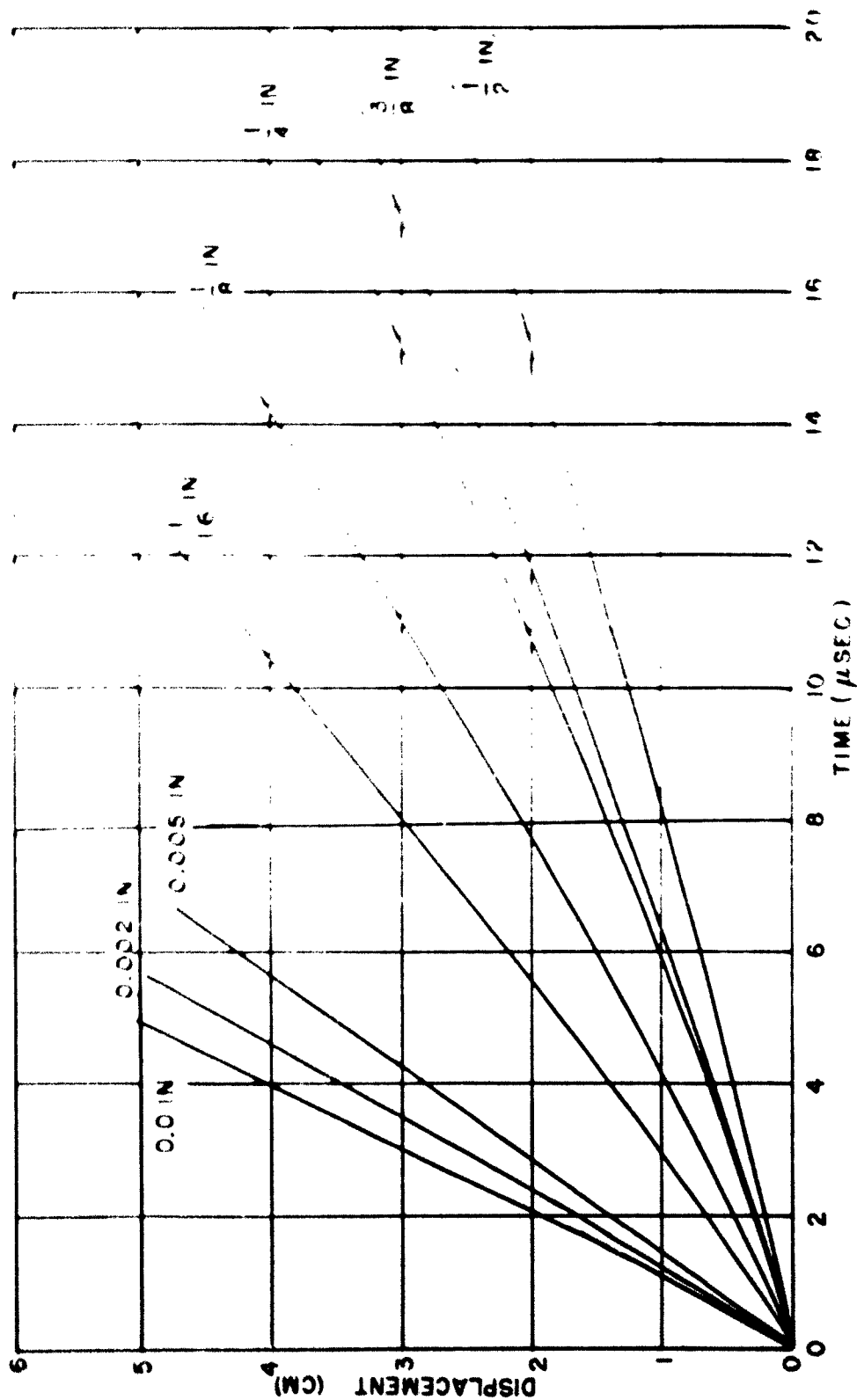


FIG. 8 AVERAGE \bar{Y} VS \bar{T} PLOT FOR EXPANSION OF ALUMINUM CYLINDERS OF VARIOUS WALL THICKNESSES

APPENDIX

ADJUSTMENT OF OBSERVED EXPANSION BECAUSE
OF REFRACTIVE INDEX CHARGES

1. In the cylinder expansion a shock wave is set up in the air in front of the expanding case. This shock travels outward at a slightly higher velocity than the cylinder as can be seen in Figures 2 and 3. The gas behind the shock front is compressed and therefore has a higher refractive index. This change of refractive index has the effect of apparently increasing the true radius of the expanding cylinder, R_1 , to an observed radius R_2 , as shown in Figure 9.

2. To obtain an estimate of the distortion the shock wave--cylinder configuration of Figure 9 is assumed. It is further assumed that the density of air and hence the refractive index behind the shock is constant and that the expansion angle of the case is small. Then it is seen that

$$\frac{R_2}{R_1} = \frac{\sin i}{\sin r} = \frac{n_2}{n_1} = n$$

$$\frac{V_A}{V_t} = \frac{dR_2/dt}{dR_1/dt} = \frac{n_2}{n_1} = n$$

where n_1 and n_2 are the refractive indices respectively in front of and behind the shock, V_A is the observed velocity, and V_t is the true velocity of the case. The Lorentz relation

$$\frac{n^2 - 1}{n^2 + 2} \cdot \frac{1}{\rho} = \text{const.}$$

will give the change in refractive index across the two regions. Assuming a refractive index of air for standard conditions (20°C, 760 mm) $n_1 = 1.00027$, then n_2 and $r = m_2/m_1$ for different values of ρ_2/ρ_1 , where ρ_2 and ρ_1 are air densities in front of and behind the shock, are as follows:

ρ_2/ρ_1	1	5	10	25	50
M_2	1.00027	1.00135	1.00270	1.00675	1.0135
M	1	1.00108	1.00243	1.0065	1.0133

Thus if p_2/p_1 is known the distortion can be obtained directly as n .

3. An upper limit to the distortion can be obtained by considering the one-dimension supersonic compressional flow example, Reference (m). This will over estimate the density increase behind the shock point because no account is taken of flow into the diverging volume elements associated with the cylindrical system, and the piston velocity in the flow example is taken considerably greater than the case velocity. In the flow example with $U_p/c \gg 1$, where U_p is the piston velocity and c is the initial velocity of sound for the gas, the shock velocity and ratio of densities, pressures, and temperatures in front of and behind the shock front are given by

$$U_{\text{shock}} \sim \frac{1}{1-\mu^2} U_p = 1.2 U_p$$

$$\frac{p_2}{p_1} \sim \frac{1}{\mu^2} = 6$$

$$\frac{\rho_2}{\rho_1} \sim \frac{1+\mu^2}{1-\mu^2} \left(\frac{U_p}{c}\right)^2 = 1.68 \left(\frac{U_p}{c}\right)^2 \sim 10 \text{ to } 40$$

$$\frac{T_2}{T_1} \sim \frac{p_2 \rho_1}{p_1 \rho_2} \sim 1.6 \text{ to } 7.$$

Here $\mu^2 = \frac{\gamma-1}{\gamma+1} = \frac{1}{6}$ for $\gamma = 1.4$ (air).

The numerical values are for U_p ranging from 2500 to 5000 feet/second. Taking only the change in density

$$\frac{p_2}{p_1} = 6 \text{ (const.)}; \quad n = 1.00137.$$

The distortion would thus be on the order of 0.1 per cent. Note, however, that the heating is considerable. The change of refractive index is not known for such a wide temperature change. Small increases in temperature of a medium at room temperature produces a decrease in its refractive index. It is assumed here

that the large temperature change does not move an absorption band of air close to the light band being observed so that the temperature effect is small. It is believed that the distortion is considerably less than 1 per cent. No refractive index correction has been made for the data.

4. It is pointed out that while a distorted radius is predicted as the cylinder just starts expanding the shock wave at this time is at the cylinder or only very little separated from it so that the observed radius is the true radius. As the cylinder starts expanding the shock wave is essentially opaque and the shock expansion itself is observed. As the compressed region becomes thicker, refracted light rays can pass over the cylinder through the shocked region beneath the shock front. The shock wave image then separates from the cylinder shadow. It is only after a "steady state" condition is reached (after transition from observing shock radius to cylinder radius) that velocity measurements can be made. Figure 10 compares the behavior of the observed cylinder radius predicted by the formula to that expected from a consideration of refraction in a shocked region with shock velocity 1.2 times cylinder velocity and an effective refractive index of 1.0065.

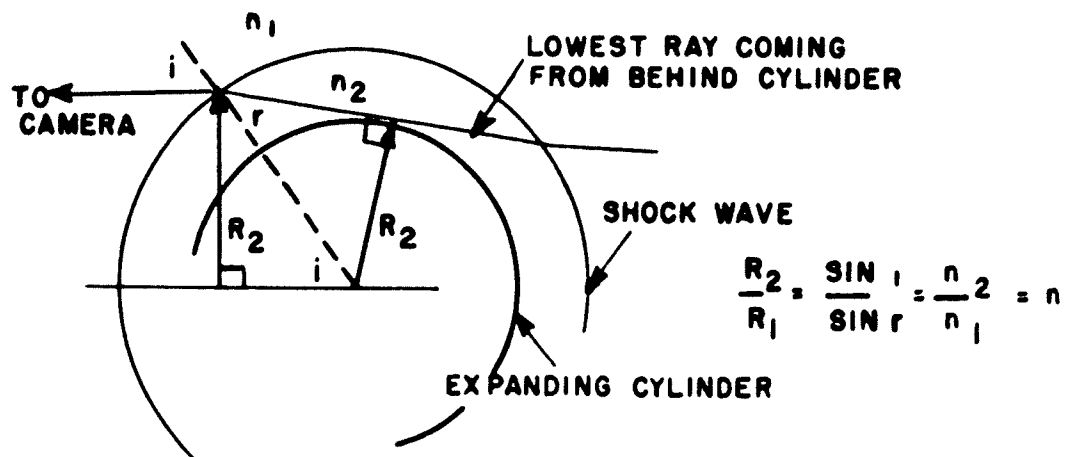


FIG.9 DISTORTION OF OBSERVED CYLINDER RADIUS
PRODUCED BY CHANGE OF REFRACTIVE INDEX

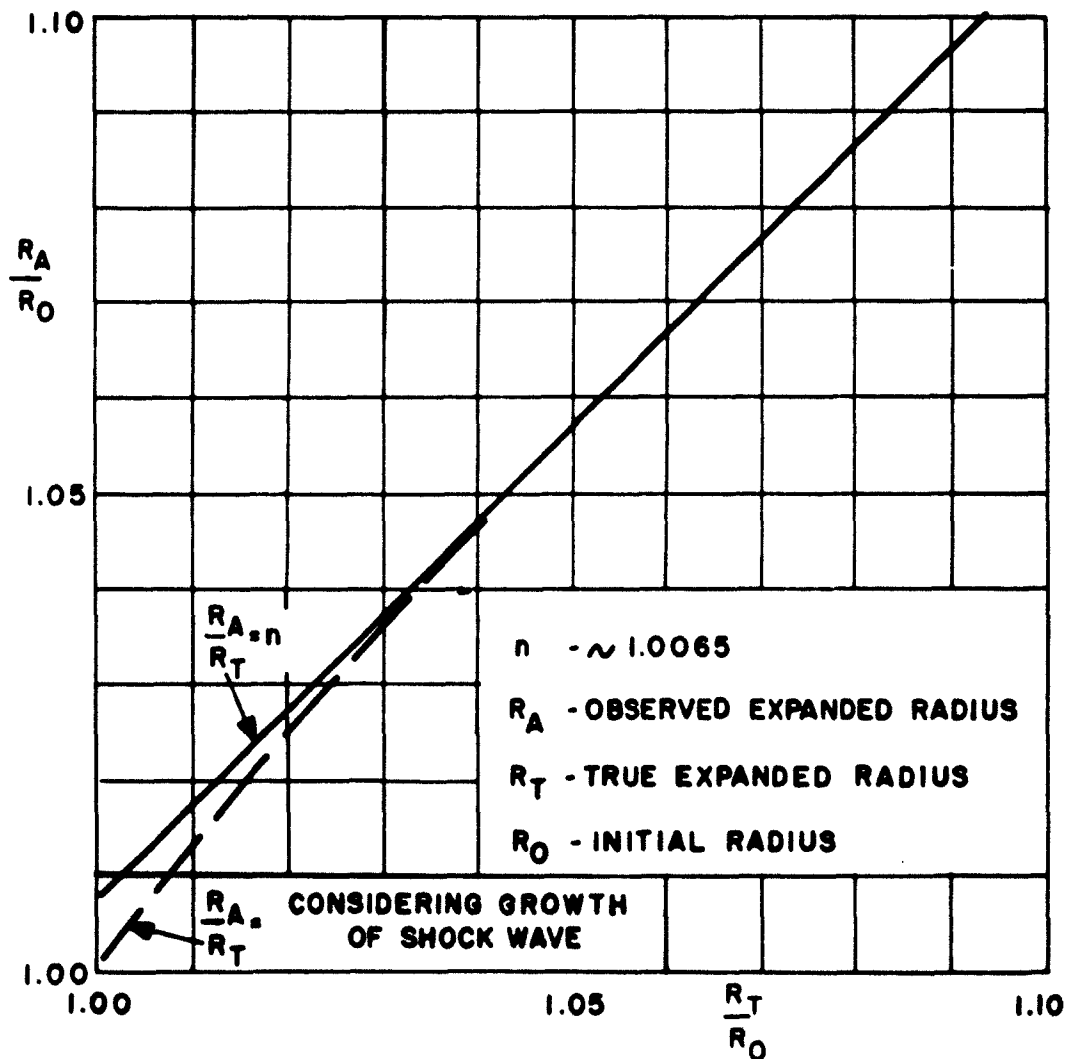


FIG. 10 THE EFFECT OF FINITE INITIAL SHOCK RADIUS ON THE DISTORTION OF THE OBSERVED CYLINDER RADIUS (U SHOCK = 1.2 U CYLINDER)

REFERENCES

- (a) R. W. Gurney. The Initial Velocities of Fragments from Bombs, Shell and Grenades. BRL Report No. 405. 14 September 1943.
- (b) G. H. Messerly. The Use of the Rotating Drum Camera for Measurement of Velocities of Shell or Bomb Fragments. OSRD Report No. 3900. 15 July 1944.
- (c) J. E. Shaw. Principles of Controlling Fragment Masses by the Grooved Ring Method. BRL Report No. 688. February 1944.
- (d) J. C. Clark. Flash Radiographs of Shell, 20 MM HEI Mk I During Static Detonation. BRL Report No. 529. 19 February 1945.
- (e) D. P. Mac Dougall and G. H. Messerly. Flash Photography of Cased Charges. Division 8, National Defense Research Council Interim Repts DFA- 1, 2, 3, etc.
- (f) G. H. Messerly. Flash Photography of Detonating Explosives. OSRD Report No. 1488. June 1943.
- (g) E. M. Boggs, R. J. Brumbaugh, and G. H. Messerly. The Application of Flash Photography to the Study of Explosion Phenomena. OSRD Report No. 5616. 27 December 1945.
- (h) S. J. Jacobs. Construction and Operation of the Rotating Mirror Camera. OSRD Report No. 5614. 11 December 1945.
- (i) D. P. Mac Dougall. A Rotating Drum Camera for the Optical Study of Detonation. OSRD Report No. 682. July 1942.
- (j) J. E. Shaw. A Measurement of the Drag Coefficient of High Velocity Fragments. BRL Report No. 744. October 1950.
- (k) T. P. Liddiard and R. D. Drosd. Exploding Wires for Light Sources in Fast Photography. NOLM Report No. 10840. 10 February 1950.
- (l) G. I. Taylor. Analysis of the Explosion of a Long Cylindrical Bomb Detonated at One End. WHSCDRD-RC Report No. 193.
- (m) W. F. Braun, A. C. Charters, and R. N. Thomas. Retardation of Fragments. BRL Report No. 425. 15 November 1943.
- (n) R. Courant and K. O. Friederichs. Supersonic Flow and Shock Waves. Interscience Publishers, New York. 1943.